Directional Character, Strength, and Nature of the Hydrogen Bond in Gas-Phase Dimers

A. C. LEGON*

Department of Chemistry, University of Exeter, Exeter EX4 4QD, U.K.

D. J. MILLEN*

Department of Chemistry, Christopher Ingold Laboratories, University College London, London WC1H 0AJ, U.K.

Received June 16, 1986 (Revised Manuscript Received October 22, 1986)

I. Introduction

During the past decade a large number of hydrogen-bonded dimers (B···HX) have been investigated in detail by rotational spectroscopy. Consequently, many properties of B···HX have been established. Because rotational spectroscopy is conducted in the gas phase at low pressure, the properties so determined refer to the isolated species B···HX. Such properties are necessarily intrinsic properties of the hydrogen-bonded dimer, free of the lattice or solvent interactions that characterize the solid or liquid phases, and provide the basis for a discussion of the interaction of B with HX without the complications encountered in condensed phases. These properties include the angular geometry of B···HX, the internuclear distances r(B···X) and r(H–X), various measures of the strength of the hydrogen bond, and the ease of angular distortion of the hydrogen bond. We shall not discuss here the rotational spectroscopy of B···HX or the methods of deriving the above properties from the observed spectra. Both of these have recently been reviewed in detail elsewhere.[1]

In this article we shall make much use of the systematic variation of B and then HX. Systematic variation of B and HX allows trends in angular geometries, in strengths of binding, in hydrogen-bond lengths, etc., to be detected and thereby provides a basis for generalizations about the hydrogen bond. We shall review such trends and the generalizations they generate. Included among the latter are an electrostatically based set of rules for predicting angular geometries, an interpretation of strengths of binding in terms of the nucleophilicity of B and the electrophilicity of HX, and a similar interpretation of the order among r(B···X) and r(H–X).

II. Angular Geometries of Hydrogen-Bonded Dimers

A Rule for Predicting Geometries. Within a few years of the first investigations of hydrogen-bonded dimers by rotational spectroscopy, two rules were enunciated which provided a method of predicting angular geometries. As further angular geometries were determined experimentally, the reliability of the rules became established. Because the rules are essentially electrostatic in nature, their experimental verification for a wide range of dimers B···HX has provided a climate of confidence for the development of electrostatic models.

We now state the rules and in the next section discuss observed dimer geometries with the rules in mind. The rules rely on the identification of nonbonding and π-bonding electron pairs (as conventionally envisaged) on the acceptor molecule B which are taken to determine the direction of the hydrogen bond. The hydrogen atom in HX is electrophilic and is assumed to seek the most electron-rich region in B. The most common electron-rich, or nucleophilic, regions will be along the axes of nonbonding or π-bonding electron pairs. Hence, the gas-phase equilibrium geometry of a dimer B···HX can be obtained from the following rules:[2]

(i) The axis of the HX molecule coincides with the supposed axis of a nonbonding electron pair as conventionally envisaged, or if B has no nonbonding electron pairs but has π-bonding pairs.

(ii) The axis of the HX molecule intersects the internuclear axis of the atoms forming the π-bond and is perpendicular to the plane of symmetry of the π-bond.

Rule i is definitive when B has both nonbonding and π-bonding pairs.

Classification of Observed Dimer Geometries according to Electron Pair Model. In the discussion that follows, we group dimers according to the number of nonbonding electron pairs carried by the acceptor atom in B. In Figures 1, 2, 4–6, and 9 we illustrate the electron pair model and the observed geometries for typical examples in each group. The diagrams involving nonbonding electron pairs are recognized to be schematic and unrealistic but have been exaggerated deliberately for convenience in applying the rules.

One Nonbonding Electron Pair on the Acceptor Atom. The three simplest acceptor molecules B that carry a single nonbonding electron pair on the acceptor atom are the isoelectronic series of linear molecules HCN, N_2, and CO. The nonbonding pairs lie along the molecular axes, as shown schematically in IA, IIA, and IIIA, respectively, of Figure 1. The rules predict for HCN···HF a linear geometry and similarly for N_2···HF. The observed geometries[3-6] are shown in IB and IIB of

A. C. Legon is Professor of Physical Chemistry in the University of Exeter. He was born in Suffolk, England, in 1941 and was educated chemically at University College London where he later held the posts of Lecturer and then Reader in the Chemistry Department. His research interests include the determination of the properties of small molecules by rotational and vibrational spectroscopy.

D. J. Millen was born in Kent in 1923. He was appointed Professor of Chemistry at University College London in 1964. His research interests are in infrared and microwave spectroscopy, particularly their application to gas-phase hydrogen bonding.

(1) Legon, A. C.; Millen, D. J. *Chem. Rev.* **1986**, *86*, 635.
(2) Legon, A. C.; Millen, D. J. *Discuss. Faraday Soc.* **1982**, *73*, 71.
(3) Legon, A. C.; Millen, D. J.; Rogers, S. C. *Proc. R. Soc. London, Ser. A* **1980**, *370*, 213.

0001-4842/87/0120-0039$01.50/0

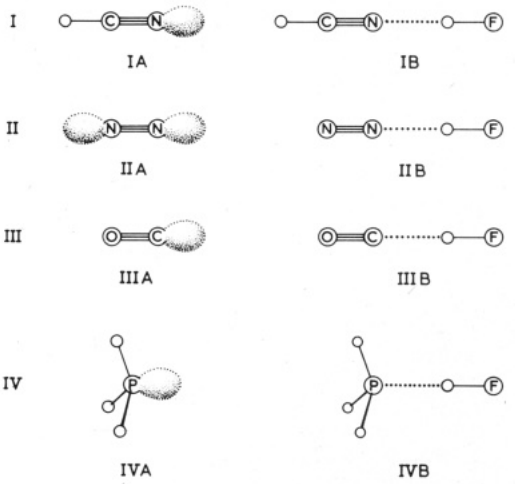

Figure 1. One nonbonding electron pair on acceptor atom: A, model showing nonbonding pair; B, observed geometry of dimer.

Figure 1 and are as predicted. When CO is the acceptor molecule, ambiguity exists in prediction of the acceptor atom, for both C and O atoms carry nonbonding pairs but, unlike those of N_2, they are not equivalent. The experimental result[7] (IIIB) establishes that the nonbonding pair on C is the more nucleophilic, in accord with the known sign of the electric dipole moment of CO. Similarly, linear geometries are predicted and observed for HCN···HCl,[8] HCN···HBr,[9] HCN···HCN,[10,11] OC···HCl,[12] OC···HBr,[13] OC···HCN,[14] N_2···HCl,[15] N_2···HCN,[16] HC≡C—C≡N···HF,[17] and NCCN···HF.[18]

Certain molecules having C_{3v} symmetry, e.g., NH_3, PH_3, CH_3CN, and $(CH_3)_3CCN$, also exhibit an axially symmetric, nonbonding electron pair, as illustrated for the example of PH_3 in IVA of Figure 1. The rules thus predict a dimer with HF which preserves the symmetry of the acceptor B. In each case, such a geometry is indeed observed,[19–24] as shown for H_3P···HF in IVB.

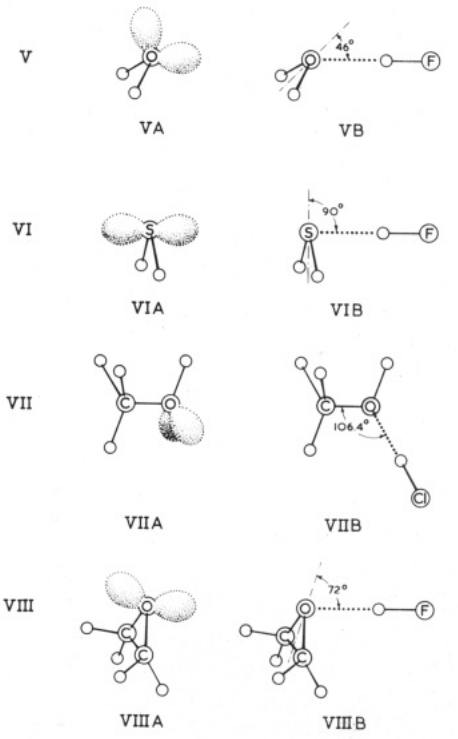

Figure 2. Two nonbonding electron pairs on acceptor atom: A, model showing nonbonding pairs; B, observed geometry of dimer.

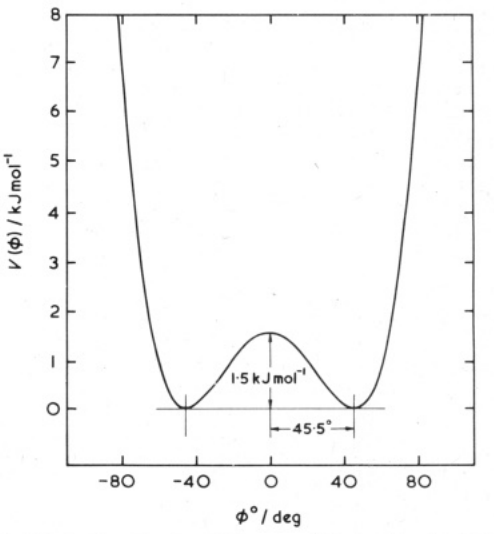

Figure 3. Variation of potential energy $V(\phi)$ with ϕ in H_2O···HF. The angle ϕ is the angle between the bisector of the ∠HOH angle and the line defined by the O···F nuclei.

Dimers of this angular geometry have also been observed[25–32] when the proton donor is variously HCl, HBr, or HCN and B is one of the above-mentioned C_{3v} species and additionally $(CH_3)_3P$.

(4) Legon, A. C.; Millen, D. J.; Willoughby, L. C. *Proc. R. Soc. London, Ser. A* **1985**, *401*, 327.
(5) Soper, P. D.; Legon, A. C.; Read, W. G.; Flygare, W. H. *J. Chem. Phys.* **1982**, *76*, 292.
(6) Legon, A. C.; Willoughby, L. C. *Chem. Phys. Lett.* **1984**, *109*, 502.
(7) Legon, A. C.; Soper, P. D.; Flygare, W. H. *J. Chem. Phys.* **1981**, *74*, 4944.
(8) Legon, A. C.; Campbell, E. J.; Flygare, W. H. *J. Chem. Phys.* **1982**, *76*, 2267.
(9) Campbell, E. J.; Legon, A. C.; Flygare, W. H. *J. Chem. Phys.* **1983**, *78*, 3494.
(10) Georgiou, K.; Legon, A. C.; Millen, D. J.; Mjöberg, P. J. *Proc. R. Soc. London, Ser. A* **1985**, *399*, 377.
(11) Campbell, E. J.; Buxton, L. W.; Flygare, W. H. *Chem. Phys.* **1981**, *56*, 399.
(12) Soper, P. D.; Legon, A. C.; Flygare, W. H. *J. Chem. Phys.* **1981**, *74*, 2138.
(13) Keenan, M. R.; Minton, T. K.; Legon, A. C.; Balle, T. J.; Flygare, W. H. *Proc. Natl. Acad. Sci. U.S.A.* **1980**, *77*, 5583.
(14) Goodwin, E. J.; Legon, A. C. *Chem. Phys.* **1984**, *87*, 81.
(15) Altman, R. S.; Marshall, M. D.; Klemperer, W. *J. Chem. Phys.* **1983**, *79*, 57.
(16) Goodwin, E. J.; Legon, A. C. *J. Chem. Phys.* **1985**, *82*, 4434.
(17) Georgiou, K.; Legon, A. C.; Millen, D. J.; North, H. M.; Willoughby, L. C. *Proc. R. Soc. London, Ser. A* **1984**, *394*, 387.
(18) Legon, A. C.; Soper, P. D.; Flygare, W. H. *J. Chem. Phys.* **1981**, *74*, 4936.
(19) Howard, B. J.; Langridge-Smith, P. R. R., to be submitted for publication.
(20) Legon, A. C.; Willoughby, L. C. *Chem. Phys.* **1983**, *74*, 127.
(21) Bevan, J. W.; Legon, A. C.; Millen, D. J.; Rogers, S. C. *Proc. R. Soc. London, Ser. A* **1980**, *370*, 239.
(22) Soper, P. D.; Legon, A. C.; Read, W. G.; Flygare, W. H. *J. Phys. Chem.* **1981**, *85*, 3440.
(23) Cope, P.; Legon, A. C.; Millen, D. J.; Willoughby, L. C. *J. Chem. Soc., Faraday Trans. 2* **1986**, *82*, 1197. Cope, P.; Legon, A. C.; Millen, D. J. *Ibid.* **1986**, *82*, 1189.
(24) Georgiou, A. S.; Legon, A. C.; Millen, D. J. *Proc. R. Soc. London, Ser. A* **1980**, *370*, 257.
(25) Fraser, G. T.; Leopold, K. R.; Nelson, Jr., D. D.; Tung, A.; Klemperer, W. *J. Chem. Phys.* **1984**, *80*, 3073.
(26) Legon, A. C.; Willoughby, L. C. *J. Chem. Soc., Chem. Commun.* **1982**, 997.
(27) Willoughby, L. C.; Legon, A. C. *J. Phys. Chem.* **1983**, *87*, 2085.
(28) Legon, A. C.; Willoughby, L. C. *Chem. Phys.* **1984**, *85*, 443.
(29) Legon, A. C.; Millen, D. J.; North, H. M., to be submitted for publication.
(30) Legon, A. C.; Willoughby, L. C. *Chem. Phys. Lett.* **1984**, *111*, 566.
(31) Howard, N. W.; Legon, A. C. *J. Chem. Soc., Faraday Trans. 2*, in press.
(32) Hirani, H. L.; Legon, A. C.; Millen, D. J.; Willoughby, L. C. *J. Mol. Struct.* **1984**, *125*, 171.

Two Nonbonding Electron Pairs on the Acceptor Atom. The simplest possible example of a donor molecule in this class is H_2O in which the oxygen atom carries two nonbonding electron pairs but in which there are no π-bonding pairs, as shown schematically in VA (Figure 2). The rules predict and experiment demonstrates[33] that $H_2O\cdots HF$ has the equilibrium angular geometry of C_s symmetry (VB in Figure 2). When there are two equivalent nonbonding pairs, the rule requires that there are two equivalent equilibrium geometries of this type. The rules tell us nothing, however, of the potential energy barrier between the two equivalent forms. In fact, by a detailed analysis of the rotational spectrum of $H_2O\cdots HF$, it has been possible to establish[33] that the potential energy barrier at the planar conformation ($\phi = 0$) is only ~ 1.5 kJ mol^{-1} above that of the pyramidal equilibrium conformers for which $\phi \approx 46°$ (see Figure 3 where the angle ϕ is also defined). The zero-point geometry is effectively planar because of the very low barrier.[34,35] Similar zero-point geometries have been observed for $H_2O\cdots HCl$[36] and $H_2O\cdots HCN$,[37,38] but these presumably have a pyramidal configuration at oxygen in the equilibrium geometry. The spectroscopically complicated dimer $H_2O\cdots HOH$ has been established[39] to have a pyramidal equilibrium arrangement at the acceptor oxygen.

We note that the equilibrium angle $\phi \approx 46°$ in $H_2O\cdots HF$ is close to the value expected given that the nonbonding pairs in H_2O are tetrahedrally disposed about the central atom, as predicted by the valence shell electron pair repulsion (VSEPR) model[40] of H_2O from an $\angle$HOH angle of 104°31′. By contrast, the $\angle$HSH angle in H_2S of 92° requires, according to the same argument, an angle ϕ of approximately 90° (see VIB in Figure 2). The L-shaped geometry predicted thereby for $H_2S\cdots HF$ with the aid of the rules is in good agreement with observation[41,42] (see VIB in Figure 2). Thus, we see the effect of varying the acceptor atom in this class. Similar shapes are observed[43–45] for $H_2S\cdots HCl$, $H_2S\cdots HBr$, and $H_2S\cdots HCN$.

The next question that arises concerns the effect of varying the groups attached to the acceptor atom. This can be illustrated by first considering methanol, which can be viewed as derived from H_2O by replacing an H atom by a CH_3 group (see VIIA in Figure 2). Although CH_3OH does not have the symmetry of H_2O, the two nonbonding pairs on O are still equivalent and the rules predict, on the basis of a tetrahedral disposition of electron pairs about O, a dimer geometry $CH_3OH\cdots HCl$ which is pyramidal at oxygen with a Cl···O–C angle of about 110°. The observed geometry[46] is shown in VIIB of Figure 2. Further substitution of CH_3 for the hydroxyl H in CH_3OH leads to dimethyl ether in which the symmetry returns to that of the water molecule. A geometry similar to that of $H_2O\cdots HF$ is thus predicted and is indeed observed[47] for $(CH_3)_2O\cdots HF$.

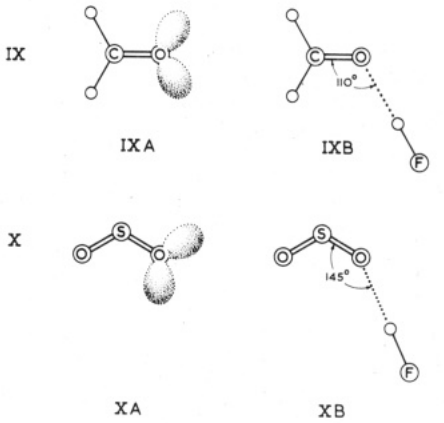

Figure 4. Two nonbonding electron pairs and one π-bonding pair on acceptor atom: A, model showing nonbonding pairs; B, observed geometry of dimer.

We have seen that, for the dimers $H_2O\cdots HF$, methanol···HCl, and $(CH_3)_2O\cdots HF$, the interbond angle at O requires, according to the VSEPR model, an approximately tetrahedral disposition of the electron pairs about oxygen, and hence the rules predict pyramidal configurations at oxygen for all three dimers. We next seek the effect on the dimer geometry of deliberately varying the interbond angle at oxygen. This can be most easily achieved by constraining the ethereal oxygen atom in a ring, first in a five-membered ring (2,5-dihydrofuran), then in a four-membered ring (oxetane), and finally in a three-membered ring (oxirane). As the size of the ring decreases, the angle $\angle$COC decreases and concomitantly the angle between the nonbonded pairs increases. This increase is reflected in the observed increase of the angle ϕ (defined in the caption to Figure 3 in the case of $H_2O\cdots HF$) from 48.5° in 2,5-dihydrofuran···HF,[48] through 57.9° in oxetane···HF,[49] to 71.8° in oxirane···HF.[50] The nonbonding pairs on oxygen in oxirane are shown schematically in VIIIA, and the observed geometry of oxirane···HF is shown in VIIIB of Figure 2.

In connection with dimers of the $R_2O\cdots HX$ type, we consider finally the variation of dimer geometry as HX is changed in order to form weaker (and longer) hydrogen bonds. From an investigation of oxirane···HCN, it has been established[51] that in changing from X = F to X = CN the angle ϕ in oxirane···HX changes from $\phi = 71.8°$ to 52.3°. The geometry has thus changed toward a planar structure, as anticipated. Nevertheless, the structure is not changed drastically from that ex-

(33) Kisiel, Z.; Legon, A. C.; Millen, D. J. *Proc. R. Soc. London, Ser. A* **1982**, *381*, 419.
(34) Beran, J. W.; Kisiel, Z.; Legon, A. C.; Millen, D. J.; Rogers, S. C. *Proc. R. Soc. London, Ser. A* **1980**, *372*, 441.
(35) Legon, A. C.; Willoughby, L. C. *Chem. Phys. Lett.* **1982**, *92*, 333.
(36) Legon, A. C.; Willoughby, L. C. *Chem. Phys. Lett.* **1983**, *95*, 449.
(37) Fillery-Travis, A. J.; Legon, A. C.; Willoughby, L. C. *Chem. Phys. Lett.* **1983**, *98*, 369.
(38) Fillery-Travis, A. J.; Legon, A. C.; Willoughby, L. C. *Proc. R. Soc. London, Ser. A* **1984**, *396*, 405.
(39) Dyke, T. R.; Muenter, J. S. *J. Chem. Phys.* **1974**, *60*, 2929.
(40) Gillespie, R. J.; Nyholm, R. S. *Q. Rev., Chem. Soc.* **1957**, *11*, 339.
(41) Viswanathan, R.; Dyke, T. R. *J. Chem. Phys.* **1982**, *77*, 1166.
(42) Willoughby, L. C.; Fillery-Travis, A. J.; Legon, A. C. *J. Chem. Phys.* **1984**, *81*, 20.
(43) Goodwin, E. J.; Legon, A. C. *J. Chem. Soc., Faraday Trans. 2* **1984**, *80*, 51.
(44) Goodwin, E. J.; Legon, A. C. *J. Chem. Soc., Faraday Trans. 2* **1984**, *80*, 1669.
(45) Jaman, A. I.; Legon, A. C., accepted for publication in *J. Mol. Struct.*
(46) Cope, P.; Legon, A. C.; Millen, D. J. *Chem. Phys. Lett.* **1984**, *112*, 59.
(47) Kisiel, Z.; Legon, A. C.; Millen, D. J.; North, H. M., to be submitted for publication.
(48) Collins, R. A.; Legon, A. C.; Millen, D. J., to be submitted for publication.
(49) Georgiou, A. S.; Legon, A. C.; Millen, D. J. *J. Mol. Struct.* **1980**, *69*, 69.
(50) Georgiou, A. S.; Legon, A. C.; Millen, D. J. *Proc. R. Soc. London, Ser. A* **1981**, *372*, 511.
(51) Goodwin, E. J.; Legon, A. C.; Millen, D. J. *J. Chem. Phys.* **1986**, *85*, 676.

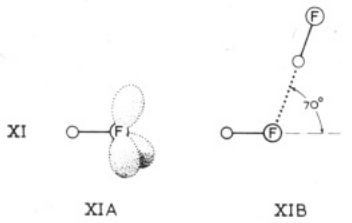

Figure 5. Three nonbonding electron pairs on acceptor atom: A, model showing nonbonding pairs; B, observed geometry of dimer.

pected in terms of the rules for predicting geometry from nonbonding electron pair directions. The geometry is, in fact, still far removed from that expected in the limit of a very long hydrogen bond when the dominance of dipole–dipole interactions will lead to a planar geometry with ϕ equal to zero (see below). The implication is that the applicability of the rules is not particularly sensitive to variation of the proton donor.

Lastly, within the class of acceptor molecules B in which the acceptor atom carries two nonbonding electron pairs, we turn to consider a subgroup exemplified by B = H_2CO and SO_2. For these molecules, the oxygen atom is also involved in a π-bond and is generally viewed as sp^2 hybridized, with nonbonding pairs occupying two of the sp^2 hybrids, as shown in IXA and XA, respectively, of Figure 4. The rule gives precedence to the *n*-type hydrogen bonds and predicts geometries in good agreement with experiment,[52-54] as illustrated in IXB and XB, respectively. Both geometries have all nuclei coplanar, in contrast to the pyramidal configuration at O in the $R_2O\cdots HX$ type dimer, as expected from the rules. However, the rules do not allow us to distinguish between the inequivalent nonbonded pairs in, for example, SO_2, that is, between the isomer of $SO_2\cdots HF$ in which the HF molecule is cis to the S=O π-bond (as in XB) and the trans form. The fact that the cis form is observed presumably means that the cis nonbonding pair is the more nucleophilic.

There are several other members of the subgroup exemplified by $H_2C{=}O$ and SO_2. Of these, $N_2O\cdots HF$ has an observed trigonal-planar arrangement at oxygen[55] like that in $H_2CO\cdots HF$. By contrast, the closely related species $OCO\cdots HF$ and $SCO\cdots HF$ have a linear arrangement, $O\cdots H{-}F$.[56] These results can be placed in context when it is noted that the hydrogen-bond stretching force constants k_σ[56] for $OCO\cdots HF$ and $SCO\cdots HF$ are comparable with those of van der Waals complexes, rather than with those of generally recognized hydrogen-bonded dimers. Indeed for (OCO,HCN) the dimer is clearly not hydrogen bonded since it has a T-shaped geometry[57] with the N atom of HCN facing the C atom of CO_2. A corresponding change in the nature of the intermolecular binding has been observed for (SO_2,HCN).[58] On the other hand, the lowest energy form of (OCS,HCN) has a linear hydrogen-bonded geometry[59] similar to that of $SCO\cdots HF$.

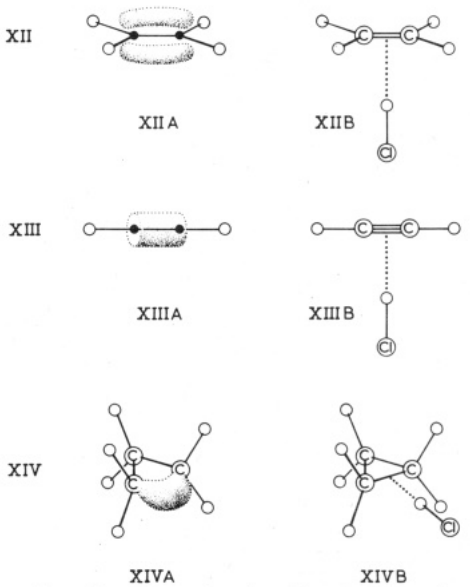

Figure 6. π-Bonding or pseudo-π-bonding electron pairs without nonbonding pairs: A, model showing π- or pseudo-π-bonding pairs; B, observed geometry of dimer.

Three Nonbonding Electron Pairs on Acceptor Atom. Only three examples have been reported in which the acceptor atom in B has three nonbonding pairs of electrons, namely, $(HF)_2$,[60] $HF\cdots HCl$,[61] and $(HCl)_2$.[62] A detailed investigation of the HF dimer and its deuteriated species establishes a nonlinear geometry in which the HF subunit acting as the proton acceptor is bent by ca. 70° from the F···F axis (see XIB in Figure 5). The electron pair model (XIA in Figure 5) predicts just such an angular geometry. An analogous nonlinear geometry holds for HF···HCl and is implied for $(HCl)_2$.

π-Bonding and Pseudo-π-Bonding Electrons on Acceptor Molecule. When π-bonding pairs but no nonbonding pairs are present on the acceptor molecule B, as in ethylene, the rules predict that in the equilibrium geometry of B···HX the axis of the HX molecule intersects the internuclear axis of the atoms forming the π-bond and is perpendicular to the plane of symmetry of the π-orbital. The familiar π-bond model for ethylene is shown in XIIA of Figure 6, and the observed geometry[63] of ethylene···HCl is shown in XIIB. The latter is as predicted by the rules.

Acetylene has two equivalent π-bonding electron pairs which have cylindrical symmetry, as conventionally represented in XIIIA of Figure 6. The rules straightforwardly lead to the T-shaped geometry shown in XIIIB for acetylene···HCl, which is as observed.[64] Acetylene is a member of the same isoelectronic series as HCN, N_2, and CO. In the dimers B···HF where B is HCN, N_2, or CO (see Figure 1) the acceptor molecule has in each case π-bonding as well as nonbonding electron pairs. In view of the linear geometry estab-

(52) Baiocchi, F. A.; Klemperer, W. *J. Chem. Phys.* **1983**, *78*, 3509.
(53) Fillery-Travis, A. J.; Legon, A. C. *Chem. Phys. Lett.* **1986**, *123*, 4.
(54) Fillery-Travis, A. J.; Legon, A. C. *J. Chem. Phys.* **1986**, *85*, 3180.
(55) Joyner, C. H.; Dixon, T. A.; Baiocchi, F. A.; Klemperer, W. *J. Chem. Phys.* **1981**, *74*, 6550.
(56) Baiocchi, F. A.; Dixon, T. A.; Joyner, C. H.; Klemperer, W. *J. Chem. Phys.* **1981**, *74*, 6544.
(57) Leopold, K. R.; Fraser, G. T.; Klemperer, W. *J. Chem. Phys.* **1984**, *80*, 1039.
(58) Goodwin, E. J.; Legon, A. C. *J. Chem. Phys.*, in press.
(59) Jaman, A. I.; Legon, A. C. *J. Mol. Struct.*, in press.
(60) Dyke, T. R.; Howard, B. J.; Klemperer, W. *J. Chem. Phys.* **1972**, *56*, 2442.
(61) Janda, K. C.; Steed, J. M.; Novick, S. E.; Klemperer, W. *J. Chem. Phys.* **1977**, *67*, 5167.
(62) Ohashi, N.; Pine, A. S. *J. Chem. Phys.* **1984**, *81*, 73.
(63) Aldrich, P. D.; Legon, A. C.; Flygare, W. H. *J. Chem. Phys.* **1981**, *75*, 2126.
(64) Legon, A. C.; Aldrich, P. D.; Flygare, W. H. *J. Chem. Phys.* **1981**, *75*, 625.

lished for each dimer, the proton evidently prefers to seek the axis of the nonbonding pair rather than the region of high π-electron density. Acetylene, on the other hand, has no nonbonding pairs and hence can form only the weaker π-bonded dimer.

Cyclopropane is well-known to behave in some ways like an unsaturated hydrocarbon. Indeed, a model which exhibits a pseudo-π-electron density and bent C–C single bonds has been proposed by Coulson and Moffitt[65] to account for such behavior. This model is shown (for one C–C bond) in XIVA of Figure 6. According to the rules, an HCl molecule would lie at equlibrium along a median of the cyclopropane equilateral triangle in order to sample the maximum pseudo-π-electron density. The observed geometry of cyclopropane···HCl is indeed just that predicted by the rules (see XIVB, Figure 6).[66]

The observed geometries[67-72] of similar dimers involving acetylene, ethylene, and cyclopropane with HF and HCN are likewise predicted by the rules. Finally, in benzene···HF and benzene···HCl, the dimers have C_{6v} symmetry with the hydrogen atom of HX probably sampling all the π-electron density.[73,74]

III. Electrostatic Nature of the Hydrogen Bond

The large number of angular geometries of hydrogen-bonded dimers discussed in section II and the success of the simple rules for predicting such geometries provide a basis for understanding the nature of hydrogen bonds. The rules are essentially electrostatic in character and rely on identification of nonbonding and π-bonding electron pair directions on the acceptor molecule B. The hydrogen atom of HX is viewed as the electrophile which seeks the direction of maximum electron density in B. The most common regions of high nucleophilicity are along the axes of nonbonding or π-bonding electron pairs. These axes are readily found with the aid of models involving either conventional hybridization or valence shell electron pair repulsion[40] (see IA to XIVA). Hence, the rules embody a *qualitative* electrostatic model. A remarkably successful *quantitative* electrostatic model has recently been proposed by Buckingham and Fowler[75,76] which incorporates a description of nonbonding pairs and of σ- and π-bonding distributions through point multipoles and leads to results which can be rationalized in a manner similar to that employed in the qualitative approach. The quantitative model has the advantage that it predicts deviations from the angles of the idealized hybridization model without invoking VSEPR. We outline below the Buckingham–Fowler model, but

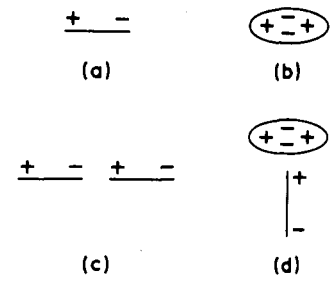

Figure 7. Diagrammatic representations of (a) a molecular dipole, (b) a molecular quadrupole, (c) a favorable relative orientation for two dipoles, and (d) a favorable orientation for a dipole and a quadrupole.

beforehand we introduce some background to the electrostatic approach.

The initial discussion will be made in terms of H_2O···HF and H_2S···HF. In the simplest electrostatic model, the electric charge distribution in the free molecules H_2O, H_2S, and HF can be viewed in terms of molecular electric dipoles only. At the next level of approximation, the charge distribution is described by a combination of electric dipole and quadrupole moments. Diagrammatically, these electric moments are shown in Figure 7a,b. At the simplest level an intermolecular attraction is therefore described as an electric dipole–electric dipole interaction, as illustrated in Figure 7c. For dimers H_2Y···HX, if the electric quadrupole moments are negligible, the arrangement in Figure 7c leads to a planar geometry. On the other hand, if the electric dipole moment of H_2Y is small while the quadrupole moment is large, the HX molecule will be aligned perpendicular to the plane of H_2Y, as illustrated in Figure 7d. To develop this simple interpretation further, the positive regions of the quadrupoles of H_2O and H_2S can be identified with hydrogen atoms and the negative regions with the nonbonding electron pairs. It turns out that the dipole moment of H_2O is almost twice that of H_2S whereas the quadrupole moment of H_2S is about $1^1/_2$ times that of H_2O. The larger dipole moment for H_2O and the larger quadrupole moment for H_2S can be rationalized by inspection of VA and VIA, respectively, in Figure 2. The L-shaped geometry of H_2S···HF with $\phi = 90°$ can then be understood in terms of the large quadrupole moment of H_2S while the smaller angle ϕ in H_2O···HF arises because of the larger ratio of dipole to quadrupole moments in H_2O by comparison with H_2S.[77] This semiquantitative model cannot be taken further, however, because of the quantitative failure of such descriptions of charge distributions when the distance between the interacting molecules is small.

In an attempt to overcome the problem of describing the interaction of charge distributions at small distances, Brobjer and Murrell[78] represented the molecular multipole moments of, for example, H_2O and HF by distributing point charges within the molecules and then evaluating the electrostatic energy of interaction among these point charges as a function of angular geometry in order to determine the most stable arrangement. Buckingham and Fowler,[76] on the other hand, represent the charge density of any particular

(65) Coulson, C. A.; Moffitt, W. E. *Philos. Mag.* **1949**, *40*, 1.
(66) Legon, A. C.; Aldrich, P. D.; Flygare, W. H. *J. Am. Chem. Soc.* **1982**, *104*, 1486.
(67) Read, W. G.; Flygare, W. H. *J. Chem. Phys.* **1982**, *76*, 2238.
(68) Shea, J. A.; Flygare, W. H. *J. Chem. Phys.* **1982**, *76*, 4857.
(69) Buxton, L. W.; Aldrich, P. D.; Shea, J. A.; Legon, A. C.; Flygare, W. H. *J. Chem. Phys.* **1981**, *75*, 2681.
(70) Aldrich, P. D.; Kukolich, S. G.; Campbell, E. J. *J. Chem. Phys.* **1983**, *78*, 3521.
(71) Kukolich, S. G.; Read, W. G.; Aldrich, P. D. *J. Chem. Phys.* **1983**, *78*, 3552.
(72) Kukolich, S. G. *J. Chem. Phys.* **1983**, *78*, 4832.
(73) Baiocchi, F. A.; Williams, J. H.; Klemperer, W. *J. Phys. Chem.* **1983**, *87*, 2079.
(74) Read, W. G.; Campbell, E. J.; Henderson, G. *J. Chem. Phys.* **1983**, *78*, 3501.
(75) Buckingham, A. D.; Fowler, P. W. *J. Chem. Phys.* **1983**, *79*, 6426.
(76) Buckingham, A. D.; Fowler, P. W. *Can. J. Chem.* **1985**, *63*, 2018.
(77) Singh, U. C.; Kollman, P. A. *J. Chem. Phys.* **1984**, *80*, 353.
(78) Brobjer, J. T.; Murrell, J. N. *J. Chem. Soc., Faraday Trans. 2* **1982**, *78*, 1853.

monomer (as obtained from accurate ab initio calculations) by point multipoles—charges, dipoles, and quadrupoles—located on each atom and in some cases at bond midpoints. These multipoles are embedded in hard van der Waals spheres which represent the short-range repulsion and determine the hydrogen-bond length at which the electrostatic interaction energy between the sets of distributed multipoles representing each monomer is to be determined. In almost all cases where an experimental structure is known this electrostatic model proves quantitatively correct. Recently, strong support for the Buckingham–Fowler model has been obtained by a comparison of its predictions with the results of ab initio calculations for a number of carefully chosen dimers.[79] The calculated interaction energy is partitioned into electrostatic, exchange, polarization, and charge-transfer contributions. The results of the calculations show that the electrostatic contribution is generally the dominant factor in determining both the strength and the directionality of the complex and that the angular dependence of the electrostatic contribution parallels that obtained from the point multipole model.

The success of the qualitative and the quantitative electrostatic models may at first sight seem surprising when it is noted that the nonbonding pairs illustrated schematicaly in the figures are enormously exaggerated and that realistic diagrams would show only a tiny deviation from a hemispherical charge distribution on, for example, the oxygen atom of H_2O.[80] This tiny deviation from a hemispherical distribution is indeed reflected in the very small difference ($\sim$1.5 kJ mol^{-1}) between the energies of the planar and equilibrium pyramidal forms of H_2O···HF (see Figure 3). Nevertheless, this deviation is clearly sufficient to define the equilibrium geometry of the isolated dimer and is therefore justifiably exaggerated in the figures.

Finally, we note that a corollary to the rules enunciated in section II provides a method of locating the axes of nonbonding electron pairs. The hydrogen bond thus acts as a probe of the directions of nonbonding pairs when these are unknown. Since the hydrogen-bond interaction is weak, the nonbonding pairs are not strongly perturbed, and consequently the concept of nucleophilicity used in this review applies essentially to the free molecule. Ab initio calculations confirm that the contribution of polarization to the energy is indeed small.[79]

IV. Strength of Hydrogen-Bonded Dimers

In this section we explore how binding strengths in a series of dimers B···HX change as B and X are varied systematically. Such binding strengths can be measured by the equilibrium dissociation energy D_e or the hydrogen-bond stretching force constant k_σ. While few experimental D_e are available,[81-83] accurate values of k_σ can now be determined[84] for a wide range of dimers B···HX, and a collection of such values for several series of dimers B···HX is given in Table I. We conclude from the table that, for any given HX, the strength of the hydrogen bond (as measured by k_σ) increases steadily along the listed series of B and so presumably does the nucleophilicity of B. On the other hand, for a given B the order of binding strength is HF > HCl > HCN $\approx$ HBr. We note that, in so far as hydrogen bonding is concerned, the electrophilicity of HX falls rapidly from HF to HCl and then decreases only slowly.

Table I.
Hydrogen-Bond Stretching Force Constants k_σ (N m^{-1}) for Series of Dimers B• • •HX Involving Nonbonding Electron Pairs[a]

B	HF	HCl	HCN	HBr
Ar	1.4[b]	1.2[c]	1.0[d]	0.8[e]
N_2	5.5[f]	2.5[g]	2.3[h]	
CO	8.5[i]	3.9[j]	3.3[k]	3.0[l]
H_3P	10.9[m]	5.9[n]	4.3[o]	5.0[p]
H_2S	12.0[q]	6.8[r]	4.7[s]	5.9[t]
HCN	18.2[u]	9.1[v]	8.1[w]	7.3[x]
CH_3CN	20.1[y]	10.7[z]	9.8[aa]	
H_2O	24.9[bb]	12.5[cc]	11.1[dd]	

[a] k_σ has been recalculated from centrifugal distortion constants in the following papers according to the appropriate expression in ref 84. [b] Dixon, T. A.; Joyner, C. H.; Baiocchi, F. A.; Klemperer, W. *J. Chem. Phys.* **1981**, *74*, 6539. [c] Novick, S. E.; Janda, K. C.; Holmgren, S. L.; Waldman, M.; Klemperer, W. *J. Chem. Phys.* **1976**, *65*, 1114. [d] Leopold, K. R.; Frazer, G. T.; Lin, F J.; Nelson, Jr., D. D.; Klemperer, W. **1984**, *81*, 4922. [e] Keenan, M. R.; Campbell, E. J.; Balle, T. J.; Buxton, L. W.; Minton, T. K.; Soper, P. D.; Flygare, W. H. *J. Chem. Phys.* **1980**, *72*, 3070. [f] Reference 6. [g] Reference 15. [h] Reference 16. [i] Reference 7. [j] Reference 12. [k] Reference 14. [l] Reference 13. [m] Reference 20. [n] Reference 26. [o] Reference 28. [p] Reference 27. [q] Reference 42. [r] Reference 43. [s] Reference 44. [t] Reference 45. [u] Reference 4. [v] Reference 8. [w] Reference 11. [x] Reference 9. [y] Reference 23. [z] Reference 29. [aa] Reference 31. [bb] Cazzoli, G.; Favero, P. G.; Lister, D. G.; Legon, A. C.; Millen, D. J.; Kisiel, Z. *Chem. Phys. Lett.* **1985**, *117*, 543. [cc] Reference 36. [dd] Reference 38.

Table II.
Hydrogen-Bond Stretching Force Constants k_σ (N m^{-1}) for Series of Dimers B• • •HX Involving π-Bonding Electron Pairs[a]

B	HF	HCl	HCN
HC≡CH		6.4[b]	5.2[c]
H_2C=CH_2		5.9[d]	4.5[e]
cyclopropane	11.5[f]	8.0[g]	6.3[h]

[a] k_σ has been recalculated from centifugal distortion constants in the following papers: [b] Reference 64. [c] Reference 70. [d] Reference 63. [e] Reference 71. [f] Reference 69. [g] Reference 66. [h] Reference 72.

The dimers B···HX in Table I all involve a hydrogen bond to a nonbonding electron pair. The corresponding set of data for series involving π-bonding pairs, i.e., B = acetylene, ethylene, and cyclopropane and HX = HF, HCl, and HCN, is displayed in Table II. We conclude that the pseudo-π-bonding pair in cyclopropane (see XIVA, Figure 6) is a better nucleophile in this situation than the π-bonds of acetylene and ethylene, presumably because of the less diffuse character of the acceptor pair in cyclopropane.

Next, in connection with the strength of binding in hydrogen-bonded dimers, we consider the resistance presented to bending the hydrogen bond. The only example where the bending force constants have been determined in detail is CH_3CN···HF.[21] Bending force constants are also available, although less well determined, for HCN···HF[3] and the "in-plane" motion of H_2O···HF.[85] In each case bending at the heavy atom

(79) Hurst, G. J. B.; Fowler, P. W.; Stone, A. J.; Buckingham, A. D. *Int. J. Quantum Chem.* **1986**, *29*, 1223.
(80) Millen, D. J. *Croat. Chem. Acta* **1982**, *55*, 133.
(81) Legon, A. C.; Millen, D. J.; Mjöberg, P. J.; Rogers, S. C. *Chem. Phys. Lett.* **1978**, *55*, 157.
(82) Thomas, R. K. *Proc. R. Soc. London, Ser. A* **1975**, *344*, 579.
(83) Pine, A. S.; Howard, B. J. *J. Chem. Phys.* **1986**, *84*, 590.
(84) Millen, D. J. *Can. J. Chem.* **1985**, *63*, 1477.
(85) Kisiel, Z.; Legon, A. C.; Millen, D. J. *J. Mol. Struct.* **1984**, *112*, 1.

Table III.
Comparison of Bond Lengths r(B• • •X) and Hydrogen-Bond Stretching Force Constants k_σ in the Series RCN• • •HF and HCN• • •HX[a]

RCN···HF			HCN···HX		
R	r(N···F)/Å	k_σ/N m^{-1}	X	r(N···X)/Å	k_σ/N m^{-1}
CN	2.895[b]	14.2[b]	F	2.805[d]	18.2[d]
HC≡C–	2.878[c]	16.3[c]	Cl	3.402[f]	9.1[f]
H	2.805[d]	18.2[d]	CN	3.331[g]	8.1[g]
CH_3	2.752[e]	20.1[e]	Br	3.609[h]	7.3[h]
			CF_3	3.488[i]	3.5[i]

[a] Bond lengths have been recalculated, where necessary, from data in the indicated reference according to the expression given in ref 4, while k_σ values have similarly been recalculated by using the appropriate expression of ref 84. [b] Reference 18. [c] Reference 17. [d] Reference 4. [e] Reference 23. [f] Reference 8. [g] Reference 11. [h] Reference 9. [i] Goodwin, E. J.; Legon, A. C. *J. Chem. Phys.* **1986**, *84*, 1988.

is relatively weakly resisted by comparison with bending at the hydrogen atom. This general finding provides a basis for understanding deviations that have been observed in the solid state from geometries predicted by the nonbonding pair model.[80,85] Analyses of large numbers of X-ray[86] and neutron[87] diffraction investigations of O···H–O bonds show that, when proper statistical weighting is applied, only a small proportion of O···H–O bonds are significantly bent at the hydrogen atom, while relatively large deviations from the tetrahedral angle at the acceptor oxygen atom are commonly observed. These results are entirely in accord with energetic considerations based on the relative magnitudes of the two bending force constants mentioned above.[85]

Finally, before leaving the topics of geometries and strengths of hydrogen-bonded dimers, which have been discussed in terms of electrostatic models, we note that objections have in fact been raised to electrostatic models[88] and a HOMO–LUMO model has been advocated.[61]

V. Bond Lengths in Hydrogen-Bonded Dimers

Two bond lengths are of interest in describing the hydrogen bond in B···HX. These are conveniently taken to be r(B···X) and r(H–X). The determination of r(B···X) by rotational spectroscopy is straightforward, and many values are available. We select two series of dimers RCN···HF and HCN···HX to illustrate the effect of changing first the nucleophilicity of B and second the electrophilicity of HX but leaving the CN group, to which the hydrogen bond is formed, unchanged. We show in Table III that in the RCN···HF series r(N···F) decreases smoothly along the series R equals CN, H, HC≡C, and CH_3, while the hydrogen-bond stretching force constant k_σ tends to increase. These orders can be taken to mean that the nucleophilicity of B increases in the order $(CN)_2$, HCN, HC≡C—CN, and CH_3CN. We also see from Table III that in the HCN···HX series the electrophilicity of HX decreases in the order X = F, Cl, CN, Br, and CF_3, as indicated by k_σ, but that the order of the r(N···X) bond lengths is determined in part by additional factors such as the effective radius of the group X.

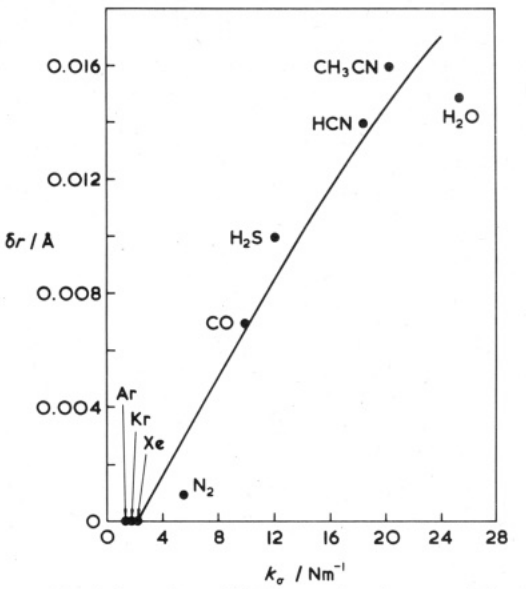

Figure 8. Variation of δr with intermolecular stretching force constant k_σ along the series B···HF, where B = Ar, Kr, Xe, N_2, CO, H_2S, HCN, CH_3CN, and H_2O.

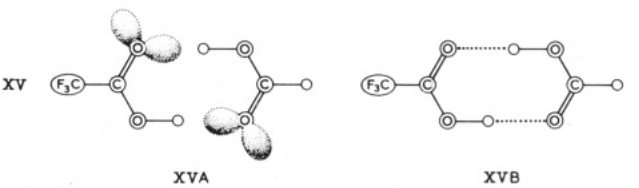

Figure 9. Carboxylic acid dimer: A, model showing nonbonding pairs; B, observed geometry of dimer.

The determination of the second bond length of interest, r(H–X), by rotational spectroscopy is less straightforward but can be achieved through a careful analysis of nuclear hyperfine structure in the spectra of B···HF dimers and has been discussed in detail elsewhere.[89] In fact, the quantity determined is the lengthening δr of the HF bond that accompanies the formation of the heterodimer B···HF. For the series B = Ar, Kr, Xe, N_2, CO, H_2S, HCN, CH_3CN, and H_2O the values of δr are found to be zero for the first three members of the series and then 0.001, 0.007, 0.010, 0.014, 0.016, and 0.015 Å, respectively. When δr is plotted against k_σ as a measure of the strength of the hydrogen bond, the result[89] is as shown in Figure 8. As the strength of binding increases, δr increases. This result can be understood qualitatively in terms of the increasing nucleophilicity of the nonbonding pair on B and its increasing local attraction for the hydrogen atom in HF and also presumably of the increasing repulsion between the end atom of B and the fluorine atom.

VI. Dimers with Two Hydrogen Bonds

The above account has been concerned with dimers involving a single intermolecular hydrogen bond. Several dimers in which there are two hydrogen bonds have also been examined by microwave spectroscopy. These include heterodimers formed by carboxylic acids,[90] e.g. (CF_3CO_2H,HCO_2H), and analogous dimers formed between carboxylic acids and amides,[91] e.g. (CF_3CO_2H,

(86) Kroon, J.; Kanters, J. A.; van Duijneveldt, J. G. C. M.; van Duijneveldt, F. B.; Vliegenthart, J. A. *J. Mol. Struct.* **1975**, *24*, 109.
(87) Ceccarelli, C.; Jeffrey, G. A.; Taylor, R. *J. Mol. Struct.* **1981**, *70*, 255.
(88) Baiocchi, F. A.; Reiher, W.; Klemperer, W. *J. Chem. Phys.* **1983**, *79*, 6428.
(89) Legon, A. C.; Millen, D. J. *Proc. R. Soc. London, Ser. A* **1986**, *404*, 89.
(90) Costain, C. C.; Srivastava, G. P. *J. Chem. Phys.* **1964**, *41*, 1620.
(91) Bellot, E. M.; Wilson, E. B. *Tetrahedron* **1975**, *31*, 2896.

CH_3CONH_2). The geometries of such dimers will be controlled to some extent by the constraint imposed by the formation of two hydrogen bonds. Nevertheless, we note that the geometry proposed for the most studied dimer (CF_3CO_2H,HCO_2H) (see XVB of Figure 9) satisfies the rules, the C═O···O angle of 120° being in accord with sp^2 nonbonding electron pairs on the carbonyl oxygen atom. It may be just because the geometry does satisfy the rules so well that carboxylic acids form such relatively strong hydrogen-bonded dimers. A quantitative estimate[90] of the binding strength in terms of the intermolecular stretching force constant implies a value of k_σ = 15.5 N m^{-1} for each O···H–O bond in (CF_3CO_2H,HCO_2H), which is indeed relatively high for a gas-phase hydrogen bond (see Table I).

VII. Concluding Remarks

The angular geometries of a wide range of hydrogen-bonded dimers in the gas phase have been rationalized on the basis of two simple rules which rely on the identification of nonbonding and π-bonding electron pairs on the acceptor molecule. The rules have been demonstrated to be electrostatic in origin. It has also been possible to understand the variation in the strength of the hydrogen bonds along series B···HX in terms of the nucleophilicity of B and the electrophilicity of HX. Moreover, the lengthening of the HX bond on formation of B···HX is shown to be simply related to the binding strength. Finally, we have indicated how the rules can be applied to understand hydrogen-bond geometries in the solid state when combined with a knowledge of bending force constants.

We are grateful to Mr. S. L. Adebayo for carrying out some calculations in connection with Tables I and II. We acknowledge support for our work on hydrogen bonding from the SERC.

Registry No. CO, 630-08-0; H_2S, 7783-06-4; HCN, 74-90-8; CH_3CN, 75-05-8; H_2O, 7732-18-5; HCl, 7647-01-0; HF, 7664-39-3; Ar, 7440-37-1; Kr, 7439-90-9; Xe, 7440-63-3; N_2, 7727-37-9.